Biomedical Optics EXPRESS

An all-fiber-optic endoscopy platform for simultaneous OCT and fluorescence imaging

Jessica Mavadia,[1,2] Jiefeng Xi,[1,2] Yongping Chen,[1] and Xingde Li[1,*]

[1]*Department of Biomedical Engineering, Johns Hopkins University, Baltimore, MD 21205, USA*
[2]*These authors contributed equally*
**xingde@jhu.edu*

Abstract: We present an all-fiber-optically based endoscope platform for simultaneous optical coherence tomography (OCT) and fluorescence imaging. This design entails the use of double-clad fiber (DCF) in the endoscope for delivery of OCT source and fluorescence excitation light while collecting the backscattered OCT signal through the single-mode core and fluorescence emission through the large inner cladding of the DCF. Circumferential beam scanning was performed by rotating a 45° reflector using a miniature DC motor at the distal end of the endoscope. Additionally, a custom DCF coupler and a wavelength division multiplexer (WDM) were utilized to seamlessly integrate both imaging modalities to achieve an entirely fiber-optically based dual-modality imaging system. We demonstrated simultaneous intraluminal 3D OCT and 2D (surface) fluorescence imaging in *ex vivo* rabbit esophagus using the dual-modal endomicroscopy system. Structural morphologies (provided by OCT) and fluorophore distribution (provided by the fluorescence module) could be clearly visualized, suggesting the potential of the dual-modality system for future *in vivo* and clinical applications.

OCIS codes: (170.4500) Optical coherence tomography; (170.2150) Endoscopic imaging; (170.6280) Spectroscopy, fluorescence and luminescence.

References and links

1. X. D. Li, S. A. Boppart, J. Van Dam, H. Mashimo, M. Mutinga, W. Drexler, M. Klein, C. Pitris, M. L. Krinsky, M. E. Brezinski, and J. G. Fujimoto, "Optical coherence tomography: advanced technology for the endoscopic imaging of Barrett's esophagus," Endoscopy **32**(12), 921–930 (2000).
2. J. M. Poneros, S. Brand, B. E. Bouma, G. J. Tearney, C. C. Compton, and N. S. Nishioka, "Diagnosis of specialized intestinal metaplasia by optical coherence tomography," Gastroenterology **120**(1), 7–12 (2001).
3. I. K. Jang, B. E. Bouma, D. H. Kang, S. J. Park, S. W. Park, K. B. Seung, K. B. Choi, M. Shishkov, K. Schlendorf, E. Pomerantsev, S. L. Houser, H. T. Aretz, and G. J. Tearney, "Visualization of coronary atherosclerotic plaques in patients using optical coherence tomography: comparison with intravascular ultrasound," J. Am. Coll. Cardiol. **39**(4), 604–609 (2002).
4. X. Li, J. Yin, C. Hu, Q. Zhou, K. K. Shung, and Z. P. Chen, "High-resolution coregistered intravascular imaging with integrated ultrasound and optical coherence tomography probe," Appl. Phys. Lett. **97**(13), 133702 (2010).
5. N. Hanna, D. Saltzman, D. Mukai, Z. Chen, S. Sasse, J. Milliken, S. Guo, W. Jung, H. Colt, and M. Brenner, "Two-dimensional and 3-dimensional optical coherence tomographic imaging of the airway, lung, and pleura," J. Thorac. Cardiovasc. Surg. **129**(3), 615–622 (2005).
6. J. J. Armstrong, M. S. Leigh, D. D. Sampson, J. H. Walsh, D. R. Hillman, and P. R. Eastwood, "Quantitative upper airway imaging with anatomic optical coherence tomography," Am. J. Respir. Crit. Care Med. **173**(2), 226–233 (2006).
7. H. O. Coxson, B. Quiney, D. D. Sin, L. Xing, A. M. McWilliams, J. R. Mayo, and S. Lam, "Airway wall thickness assessed using computed tomography and optical coherence tomography," Am. J. Respir. Crit. Care Med. **177**(11), 1201–1206 (2008).
8. R. Huber, M. Wojtkowski, and J. G. Fujimoto, "Fourier Domain Mode Locking (FDML): A new laser operating regime and applications for optical coherence tomography," Opt. Express **14**(8), 3225–3237 (2006).
9. J. F. de Boer, B. Cense, B. H. Park, M. C. Pierce, G. J. Tearney, and B. E. Bouma, "Improved signal-to-noise ratio in spectral-domain compared with time-domain optical coherence tomography," Opt. Lett. **28**(21), 2067–2069 (2003).
10. R. S. Dacosta, B. C. Wilson, and N. E. Marcon, "New optical technologies for earlier endoscopic diagnosis of premalignant gastrointestinal lesions," J. Gastroenterol. Hepatol. **17**(Suppl), S85–S104 (2002).

#175360 - $15.00 USD Received 7 Sep 2012; revised 15 Oct 2012; accepted 15 Oct 2012; published 16 Oct 2012

11. R. Kiesslich, J. Burg, M. Vieth, J. Gnaendiger, M. Enders, P. Delaney, A. Polglase, W. McLaren, D. Janell, S. Thomas, B. Nafe, P. R. Galle, and M. F. Neurath, "Confocal laser endoscopy for diagnosing intraepithelial neoplasias and colorectal cancer *in vivo*," Gastroenterology **127**(3), 706–713 (2004).
12. J. K. Barton, F. Guzman, and A. Tumlinson, "Dual modality instrument for simultaneous optical coherence tomography imaging and fluorescence spectroscopy," J. Biomed. Opt. **9**(3), 618–623 (2004).
13. S. A. Yuan, C. A. Roney, J. Wierwille, C. W. Chen, B. Y. Xu, G. Griffiths, J. Jiang, H. Z. Ma, A. Cable, R. M. Summers, and Y. Chen, "Co-registered optical coherence tomography and fluorescence molecular imaging for simultaneous morphological and molecular imaging," Phys. Med. Biol. **55**(1), 191–206 (2010).
14. Y. B. Zhao, B. W. Graf, E. J. Chaney, Z. Mahmassani, E. Antoniadou, R. Devolder, H. Kong, M. D. Boppart, and S. A. Boppart, "Integrated multimodal optical microscopy for structural and functional imaging of engineered and natural skin," J Biophotonics **5**(5-6), 437–448 (2012).
15. R. A. Wall, G. T. Bonnema, and J. K. Barton, "Focused OCT and LIF endoscope," Proc. SPIE **7558**, 75580Q (2010).
16. H. Yoo, J. W. Kim, M. Shishkov, E. Namati, T. Morse, R. Shubochkin, J. R. McCarthy, V. Ntziachristos, B. E. Bouma, F. A. Jaffer, and G. J. Tearney, "Intra-arterial catheter for simultaneous microstructural and molecular imaging *in vivo*," Nat. Med. **17**(12), 1680–1684 (2011).
17. J. Mavadia, J. Xi, Y. Chen, and X. Li, "All-fiber-optic based catheter system for simultaneous endoscopic optical coherence tomography and fluorescence imaging," in *Biomedical Optics*, OSA Technical Digest (Optical Society of America, 2012), paper BTu4B.7.
18. G. J. Tearney, S. A. Boppart, B. E. Bouma, M. E. Brezinski, N. J. Weissman, J. F. Southern, and J. G. Fujimoto, "Scanning single-mode fiber optic catheter-endoscope for optical coherence tomography," Opt. Lett. **21**(7), 543–545 (1996).
19. H. L. Fu, Y. X. Leng, M. J. Cobb, K. Hsu, J. H. Hwang, and X. D. Li, "Flexible miniature compound lens design for high-resolution optical coherence tomography balloon imaging catheter," J. Biomed. Opt. **13**(6), 060502 (2008).
20. P. H. Tran, D. S. Mukai, M. Brenner, and Z. P. Chen, "*In vivo* endoscopic optical coherence tomography by use of a rotational microelectromechanical system probe," Opt. Lett. **29**(11), 1236–1238 (2004).
21. P. R. Herz, Y. Chen, A. D. Aguirre, K. Schneider, P. Hsiung, J. G. Fujimoto, K. Madden, J. Schmitt, J. Goodnow, and C. Petersen, "Micromotor endoscope catheter for *in vivo*, ultrahigh-resolution optical coherence tomography," Opt. Lett. **29**(19), 2261–2263 (2004).
22. J. F. Xi, L. Huo, Y. C. Wu, M. J. Cobb, J. H. Hwang, and X. D. Li, "High-resolution OCT balloon imaging catheter with astigmatism correction," Opt. Lett. **34**(13), 1943–1945 (2009).
23. Y. C. Wu, J. F. Xi, L. Huo, J. Padvorac, E. J. Shin, S. A. Giday, A. M. Lennon, M. I. F. Canto, J. H. Hwang, and X. D. Li, "Robust high-resolution fine OCT needle for side-viewing interstitial tissue imaging," IEEE J. Sel. Top. Quantum Electron. **16**(4), 863–869 (2010).
24. G. J. Tearney, M. E. Brezinski, B. E. Bouma, S. A. Boppart, C. Pitris, J. F. Southern, and J. G. Fujimoto, "*In vivo* endoscopic optical biopsy with optical coherence tomography," Science **276**(5321), 2037–2039 (1997).

1. Introduction

Optical coherence tomography (OCT) is a high resolution, non-invasive and non-contact biomedical imaging modality, capable of visualizing the microstructure of biological tissue in real time. The development of innovative endoscopes enable OCT imaging of a variety of internal luminal organs such as the gastrointestinal tract [1,2], coronary arteries [3,4], and the respiratory tract [5–7]. Recent developments in Fourier-domain OCT (FD-OCT) technologies including swept-source OCT (SS-OCT) and spectral domain OCT (SD-OCT) have led to significant increases in imaging speed [8,9].

While OCT is able to provide high resolution morphological information with high speed, one caveat is its lack of molecular sensitivity, which, can be crucial for drawing conclusions for diagnosis. Conventionally, fluorescence imaging has been used to obtain molecular information. One example is endoscopic fluorescence imaging of the gastrointestinal track for cancer screening/diagnosis [10], where, generally only surface images with low resolution are generated without depth-resolved high-resolution tissue microstructure information. Another example is the emerging fluorescence confocal endomicroscopy technology [11], where, with the help of intravenously administered fluorescein, tissue microstructures with a superb resolution comparable to histology can be viewed; however the image depth and field of view are both limited.

Thus, there is a critical need to move towards multi-modality imaging to visualize tissue microstructure with high resolution and gain molecular information at the same time. In this paper, we focus on integrating OCT with fluorescence imaging seamlessly in an endoscopic setting. The combination of OCT and fluorescence imaging has shown to be effective in visualizing morphology and fluorophore distribution in bench-top systems [12–14].

#175360 - $15.00 USD Received 7 Sep 2012; revised 15 Oct 2012; accepted 15 Oct 2012; published 16 Oct 2012

Performing dual-modality optical imaging of internal luminal organs requires endoscope based imaging probes. A couple of designs for dual-modal endoscopes have been proposed and demonstrated. One design used multiple optical fibers with one for sending/receiving OCT source/backscattered light, another for delivery fluorescence excitation and a third for collecting fluorescence emission [15]. Another design used double-clad fiber (DCF) in conjunction with a fiber-optic rotary joint to construct an endoscope probe [16].

In this paper, we report an all-fiber-optic, distal end scanning, DCF-based endoscope system for seamlessly integrated simultaneous OCT and fluorescence imaging. Circumferential beam scanning is achieved through the use of a DC micromotor at the distal end of the endoscope which avoids the challenges in engineering a high-performance DCF rotary joint with required low cross-talk between OCT and fluorescence channels. The all-fiber-optic design entails the use of a wavelength division multiplexer (WDM), which significantly improved coupling efficiency of OCT source light and the overall system signal to noise ratio (SNR) by 6dB (compared to a system using a fiber-optic coupler to combine and separate OCT source and fluorescence excitation light). Proof-of-concept imaging experiments using the all-fiber-optic dual-modality endoscopic imaging system, based upon on our initial design reported at OSA Biomed Conference [17], have been performed. The feasibility of this system has been demonstrated by intraluminal imaging of *ex vivo* rabbit esophagus, where normal layered structures and glands could be clearly revealed with OCT while superficial vascular structures could be simultaneously visualized through fluorescence imaging.

2. Methods

One major consideration in the development of a dual-modality imaging system lies in the ability to simultaneously perform OCT and fluorescence imaging without compromising image quality or causing one modality to interfere with the other. One approach is to design an endoscope that can be shared by both imaging modalities. Here, we propose an endoscope which consists of a single DCF, where the single-mode core is used for OCT imaging and the large inner cladding (as well as the core) for fluorescence imaging. Beam scanning is achieved at the distal end of the probe with an ultra-compact, computer-controlled micromotor. The use of a single DCF in the endoscope ensures that the entire probe is flexible and compact. From the system level, however, more challenges remain to be solved, including efficient coupling the OCT source light with the fluorescence excitation light, and effective separation of the backscattered OCT light and the fluorescence signal without compromising the SNR for either of the imaging modalities. In the following, we will present the details of the endoscope design and then proceed to describe an all-fiber-optic platform that seamlessly integrates both imaging modalities while significantly reducing any potential SNR drop for either imaging modality. Finally, we will discuss the experiments executed to test the performance of the dual-modal endoscopic imaging system using *ex vivo* tissues.

2.1. System architecture

The overall system schematic of the fully integrated dual-modality imaging platform is shown in Fig. 1. In essence, it consists of two modules, an OCT module and a fluorescence imaging module. The two modules are combined in the OCT sample arm through a dual-modal endoscope and several customized fiber-optic components. The OCT module consists of a swept-source which is a home-built 40 kHz Fourier-domain mode-locking (FDML) fiber laser operating at a center wavelength of 1305 nm with a 3dB spectral bandwidth of ~140 nm. The OCT module also includes a Mach-Zehnder interferometer (MZI) to generate a calibration signal and a dual-balanced detector is utilized. The fluorescence imaging module consists of an argon ion laser at 488 nm for excitation and a photomultiplier tube (PMT) for detection. In order to block the leakage from the excitation light source, band-pass filters are placed in front of the PMT.

#175360 - $15.00 USD Received 7 Sep 2012; revised 15 Oct 2012; accepted 15 Oct 2012; published 16 Oct 2012

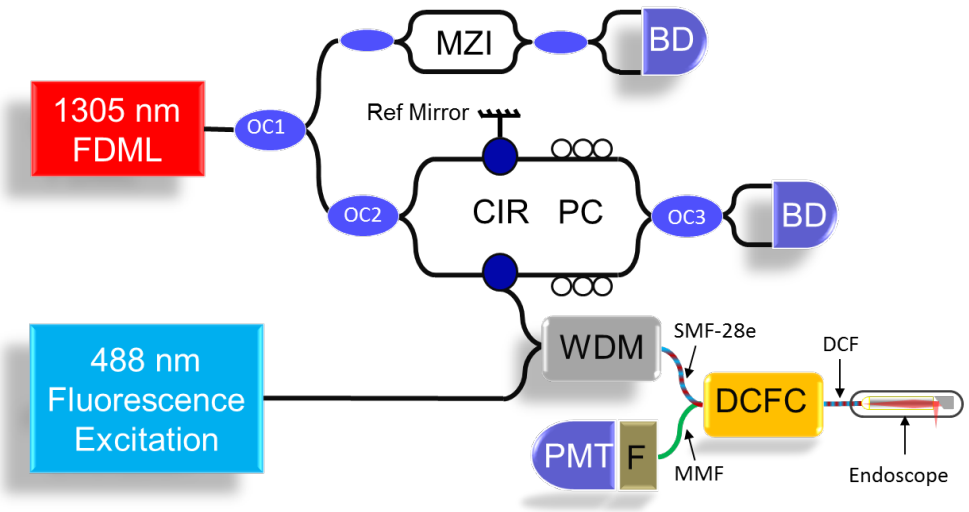

Fig. 1. Schematic of the dual-modality system capable of performing endoscopic OCT and fluorescence imaging simultaneously. FDML: Fourier-domain mode-locking fiber laser; OC: Optical coupler (OC1 95/5, OC2 70/30, OC3 50/50); MZI: Mach-Zehnder interferometer; CIR: Circulator; PC: Polarization controller; BD: Balanced detector; WDM: Wavelength division multiplexer; DCFC: double-clad fiber coupler; PMT: Photomultiplier tube; F: Bandpass filter; Green: Multimode fiber (MMF); Blue/Red: Double-clad fiber (DCF); Black: Single-mode fiber (SMF-28e).

2.2. Dual-modal imaging endoscope

One key challenge in the development of the dual-modality imaging system was in the endoscope. There were several design challenges, and the key design considerations include efficient delivery of the OCT source light and fluorescence excitation light, effective collection of OCT backscattered light in single mode, effective collection of fluorescence emission, and implementation of a scanning mechanism with a compact footprint.

In order to solve the first challenge and maintain a single fiber based design with a small overall probe diameter and high collection efficiency, we chose to use a custom double-clad fiber (DCF) with a 9 μm diameter core, 180 μm diameter inner cladding and 200 μm diameter outer cladding. The core ensures single-mode transmission for the 1305 nm OCT light source while guiding fluorescence excitation in multimode. Upon recollection, the backscattered OCT light, fluorescence emission and excitation light travel through the core and inner cladding of the DCF.

The second consideration was the implementation of a scanning mechanism. Typically circumferential beam scanning in side-viewing endoscopes has been realized either by using a fiber-optic rotary joint at the proximal end of the endoscope [18,19], or by scanning the beam through a micromotor at the distal end [20,21]. Although a fiber-optic rotary joint could be used in principle for rotating the dual-modal DCF-based endoscope, a custom rotary unit made of DCF would be needed. This approach, however, requires extremely precise alignment within the rotatory joint over 360-degree rotation in order to prevent the backscattered OCT light traveling in the inner cladding of the endoscope from being coupled into the single-mode fiber in the interferometer. This light would otherwise significantly comprise the OCT image quality (considering the light traveling in the inner cladding of the endoscope experiences different optical pathlengths from the OCT backscattered light traveling in the single-mode core). For these reasons, we adopted the distal end beam scanning approach. For proof-of-concept, an off-the-shelf ϕ1.9 mm DC micromotor was used. A 45-degree microreflector was glued onto the shaft of the micromotor and rotated in order to perform circumferential beam scanning.

#175360 - $15.00 USD Received 7 Sep 2012; revised 15 Oct 2012; accepted 15 Oct 2012; published 16 Oct 2012

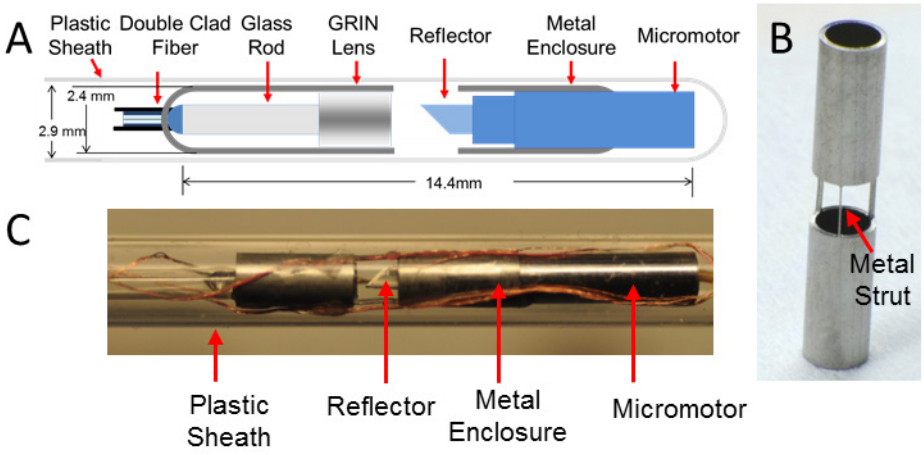

Fig. 2. (A) Schematic of distal end of the dual-modal endoscope design. (B) Photograph of a precision-cut metal enclosure (of an outer diameter 2.4 mm) with minimal beam blockage (i.e., less than 5%). (C) A photograph of the constructed endoscope of an overall diameter of 2.9 mm including the housing transparent sheath.

The overall endoscope optics design was similar to the one published in the earlier papers [19,22,23]. A glass rod was used after the DCF to expand the beam prior to focusing with a gradient index (GRIN) lens as shown in Fig. 2(A). Considering the fiber and lens assembly and the micromotor and microreflector assembly are separate from each other at the distal end of the probe, special care needs to be taken for precise alignment, centering, and stabilization of the two assemblies. A metal enclosure was fabricated from a 13 gauge hypodermic tube that was able to easily house the micromotor. As shown in Fig. 2(B), the enclosure consisted of three windows separated by ultrathin metal struts (~127 μm wide). Three struts provided sufficient mechanical stability while minimizing blockage to the imaging beam (i.e., only 5% of the view over 360 degrees was blocked). The microreflector attached to the micromotor shaft was positioned in the middle of the window within the housing tube, which deflected the imaging beam from the GRIN lens by ~90° to the sample.

The working distance of the endoscope, defined as the distance between the focal point and the surface of the metal enclosure, was governed by the GRIN lens and is able to be adjusted by the separation between the GRIN lens and the microreflector, and it was measured to be about 1.9 mm. The measured lateral resolution of the endoscope was ~13.7 μm. The distal end of the probe has an overall diameter of 2.4 mm and a rigid length of 14.4 mm. For practical use, the entire endoscope was encased in an off-the-shelf transparent plastic sheath (of an outer diameter ~2.9 mm). It is noted that the extra benefit of the distal end scanning approach is the ease in setting the desired focal position outside the plastic sheath, e.g., by adjusting the separation between the microreflector and the fiber-lens assembly. In our case, the beam focus was set at about 1.6 mm outside the sheath.

2.3. Combination of OCT source light and fluorescence excitation light

The next associated challenge in the dual-modal system was the combination of OCT source light and fluorescence excitation light. There are several ways of combining the source light, e.g., by using free-space optics, a fiber-optic coupler, or other fiber-optic methods. Since the OCT backscattered light will also go through the coupling device, it is critical to keep the round-trip loss low for the coupling unit. In our approach (see Fig. 1) we chose to use a specialized fiber-optic wavelength division multiplexer (WDM) which works for both the near infrared OCT source wavelength around 1305 nm and the visible fluorescence excitation light around 488 nm. The WDM allowed us to obtain a minimal insertion loss (i.e., 0.5 dB) for OCT as compared to free space coupling or the use of a simple fiber-optic coupler, which would have resulted in a significant roundtrip loss (i.e., more than 6 dB) and thus degrading

#175360 - $15.00 USD Received 7 Sep 2012; revised 15 Oct 2012; accepted 15 Oct 2012; published 16 Oct 2012

OCT detection sensitivity. Due to the large separation between the OCT and fluorescence source wavelengths, the efficiency of the WDM for transmitting the fluorescence excitation light (488 nm) was sub-optimal, which was ~60%. Nonetheless this efficiency was sufficient and 3 mW incident power of fluorescence excitation light was easily achievable at the sample surface, which was sufficient for fluorescence imaging.

2.4. Separation of OCT and fluorescence excitation light

The final challenge in this system lay in separating the backscattered OCT light from the fluorescence emission light that were both collected by and transmitted through the endoscope on the return path. While the most straight-forward way to separate the two signals is to use free-space optics involving collimators and a dichroic mirror (schematic not shown), recoupling the OCT signal back to a single-mode fiber in the interferometer would introduce extra loss and thus degrade the OCT detection sensitivity. In addition, the use of free-space optics would also sacrifice the portability and stability of the system. Our solution was to use a custom DCF coupler, which was able to separate the light in the inner cladding and the light in the core of the DCF and direct the light into two separate paths. The DCF coupler consists of a single-mode fiber (SMF-28e) port, a DCF port, and a multimode fiber port (see Fig. 1).

On the forward path (from the source to the sample), the DCF coupler allows the both OCT source and fluorescence excitation light traveling through the single-mode fiber to be coupled into the single-mode core of the DCF port (with a loss of 0.8dB and 2.2 dB, respectively). On the return path (from the sample back to the detector), the OCT backscattered light and fluorescence emission travel through both the core and inner cladding of the DCF in the endoscope and the DCF coupler. The light traveling in the core of the DCF is coupled back to the single-mode fiber port and the light traveling in the inner cladding is separated into the multimode fiber port (with 5dB loss for the fluorescence light). In this way the OCT backscattered light is able to return to the OCT system seamlessly through fiber optics, where balanced detection is performed and only light at the OCT source wavelength can pass through the circulator to interfere with light from the OCT reference arm at the detector. The fluorescence emission, which travels mostly through the inner cladding, was coupled into the multimode fiber port of the DCF coupler and was then detected by a photomultiplier tube (PMT). In order to minimize potential leakage of the fluorescence excitation light that was backscattered into the endoscope and transmitted through the inner cladding, bandpass filters were placed before the PMT. Both the detected OCT and fluorescence signals were digitized, displayed and stored in computer in a synchronized fashion.

3. Results

In order to test the feasibility of this dual-modality system we performed simultaneous intraluminal OCT and fluorescence imaging using *ex vivo* rabbit esophagus.

3.1. Intraluminal imaging

We tested the feasibility of the dual-modal endoscope for intraluminal imaging using rabbit esophagus. The entire intact *ex vivo* rabbit esophagus was obtained fresh from other irrelevant experiments. The tissue was stained through 3 local injections (offset by 1 cm along the length of the esophagus) with 1-2 mL of a 300 μM solution of fluorescein sodium at each location. The dye solution was injected between the lamina propria and muscularis mucosa from the submucosal side. The tissue was then rinsed with buffered saline to get rid of excess dyes.

The endoscope was deployed into the esophagus for circumferential imaging. To provide a registration landmark for both OCT and fluorescence as well as stabilize the tissue, the tissue was sutured to the transparent plastic sheath of the endoscope. Simultaneous 3D volumetric OCT imaging and 2D fluorescence imaging were achieved by scanning the imaging beam circumferentially with the micromotor while pulling back the entire endoscope within the stationary plastic sheath. OCT imaging was performed at a speed of 40,000 A-scans per second, with each circumferential frame consisting of 4,096 A-scans and each A-scan of 2048

#175360 - $15.00 USD Received 7 Sep 2012; revised 15 Oct 2012; accepted 15 Oct 2012; published 16 Oct 2012

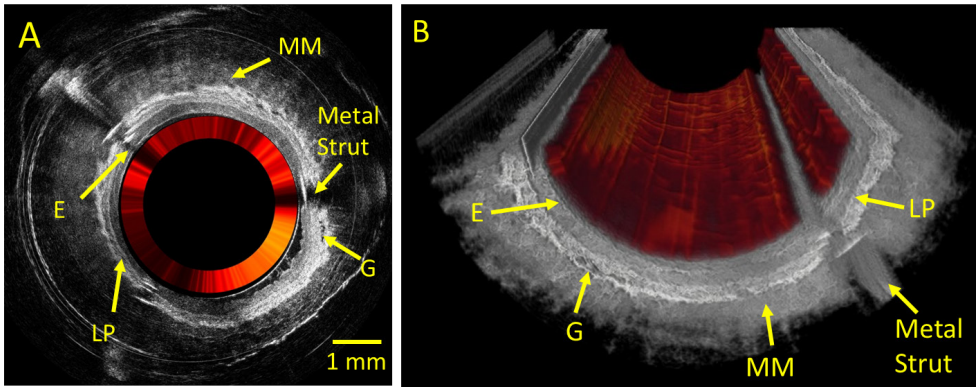

Fig. 3. Circumferential scanning and pull back were performed to obtain 3D volumetric OCT images and 2D fluorescence surface map of the esophagus with the endoscope. (A) Representative 2D cross-sectional OCT image of *ex vivo* rabbit esophagus during one circumferential scan (grayscale) with the overlaid inner annulus (red hot color map) of the fluorescence intensity. (B) The cut-away view of the 3D OCT volumetric image (grayscale) and the 2D fluorescence intensity map inlaid (red hot color map) on top of the OCT image. In both the 2D OCT cross-sectional image and 3D volumetric OCT image the normal layered structures of the esophagus can be clearly visualized, including the epithelium (E), lamina propria (LP), muscularis mucosa (MM), and glands (G). The co-registered and simultaneously acquired fluorescence map shows striated structures which are believed to be vasculature [24].

pixels. The circumferential frame rate was 10 frames per second which was limited by the gearhead on the off-the-shelf DC micromotor. For fluorescence surface imaging, each circumferential image consisted of 4096 pixels. The endoscope pull-back speed was 0.2 mm/second, corresponding to a pitch (i.e., the distance between two adjacent circumferential frames) of 20 µm.

With the above imaging parameters, it took about 30 seconds to image the esophagus over a 6 mm long segment. Figure 3(A) shows a representative cross-sectional OCT image in grayscale from one circumferential pull-back scan and the colored annulus (red hot color map) superposed on top of the OCT image depicts the fluorescence intensity over one circumferential (360 degree) rotation. Figure 3(B) shows a longitudinally cut-away view of the 3D volumetric OCT image of the 6 mm long rabbit esophagus segment, while the 2D fluorescence intensity map is inlaid on the inner surface of the OCT 3D image. Figure 3 allows visualization of normal esophageal structures (epithelium, lamia propria, muscularis mucosa and glands) in the OCT cross-sectional image as well as 3D volumetric image. Complementary to the OCT images, the inlaid 2D fluorescence intensity map displays striated structures along the length of the esophagus which are believed to be vascular structures rabbit esophagus [24]. Additionally, the coincidence and co-registration of the OCT image and fluorescence intensity image can be seen at the three signal poor points corresponding to the three metal struts of the housing enclosure.

These experiments demonstrated the ability of the endoscope to perform intraluminal imaging along the length of the esophagus. Both OCT and fluorescence intensity were able to be captured simultaneously and were automatically co-registered. The endoscope was able to image with an OCT detection sensitivity of ~108 dB and a penetration depth ~1.7 mm to reveal the normal microstructure of rabbit esophagus while simultaneously gathering fluorescence intensity.

3.2. OCT-fluorescence correlation

In order to correlate both sets of data, the intraluminal OCT tomogram was flattened into a 2D stack along imaging depth, and the unwrapped 2D fluorescence map and three representative OCT slices 700µm apart in depth are shown in Fig. 4. The structures indicated by the white arrows on the OCT slices (Figs. 4(B)-4(C)) correspond to the black arrows seen in the

#175360 - $15.00 USD Received 7 Sep 2012; revised 15 Oct 2012; accepted 15 Oct 2012; published 16 Oct 2012

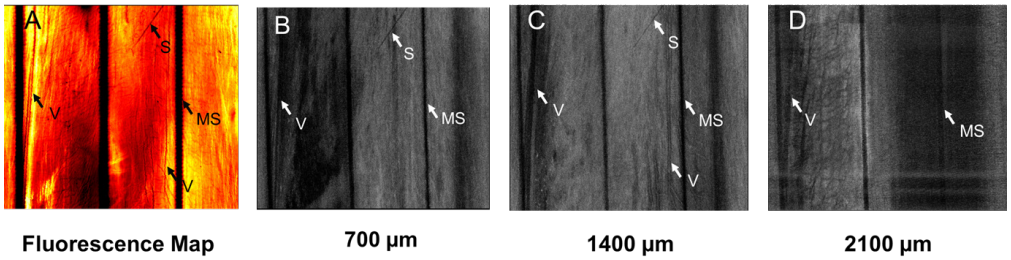

Fig. 4. (A) Unwrapped 2D Fluorescence image. (B-D) Unwrapped OCT images at 700 µm, 1400 µm, and 2100 µm depth. The white arrows on the OCT images (B-D) correspond to the black arrows in the fluorescence map (A) indicating correlating structures such as vasculature (V), suture (S), and metal strut (MS). The suture was used to provide a registration mark for both OCT and fluorescence intensity images.

fluorescence map (Fig. 4(A)). We were able to visualize the suture used as a registration mark; striated structures that are believed to be vasculature through the length of the esophagus, and the metal struts which are the signal poor regions in both the OCT and fluorescence intensity images. While both OCT and fluorescence are able to visualize the suture and vascular structures, individually, the OCT volumetric image (as seen in Figs. 3(A)-3(B)) shows additional microstructure (epithelium, lamina propria, muscularis mucosa, and glands). Furthermore, with the use of other fluorescent molecular contrast agents the fluorescence imaging mode could potentially reveal disease specific information, otherwise unseen by OCT.

4. Discussion and conclusion

The dual-modality endoscope system was able to perform intraluminal imaging of rabbit esophagus *ex vivo*. OCT allowed visualization of several layers of tissue such as the epithelium, lamina propria, muscularis mucosa as well as glands. In the fluorescence imaging system through the use of exogenous fluorophores we could visualize vascular structures along the esophagus. Although there are many fluorophores available, we opted for fluorescein sodium as the chosen dye for intraluminal imaging due to its widespread clinical use.

The system was able to achieve an OCT detection sensitivity of ~108 dB with an imaging speed of 40,000 A-scans per second for simultaneous intraluminal OCT and fluorescence imaging. This system was able to acquire automatically co-registered images as seen from the *ex vivo* rabbit esophagus experiments without sacrificing any imaging speed, suggesting the potential ability of this endoscope to be used for *in vivo* applications.

The current proof-of-concept endoscope has a diameter ~2.4 mm, and with a transparent sheath, the overall diameter is 2.9 mm which is slightly larger than the 2.8 mm accessory port of a commonly used clinical gastroscope. The current endoscope diameter is simply governed by the size of the off-the-shelf micromotor we have in the lab. The endoscope diameter, however, can be conveniently reduced by almost 50% by using a newly available micromotor which has a diameter only about 1 mm.

In conclusion, we have developed and demonstrated a dual-modality all-fiber-optic endoscope system for simultaneous OCT and fluorescence imaging. The dual-modality endoscope was based upon DCF and distal end beam scanning through a 1.9 mm DC micromotor. The system has been maintained as entirely fiber-optic through the use of a WDM for combining OCT source light and fluorescence excitation light, and a custom DCF coupler for effectively separating OCT backscattered light from fluorescence emission. The seamless, all-fiber-optic dual-modal system design significantly improved the OCT signal-to-noise ratio by more than 6 dB (compared to a system using a fiber-optic coupler to combine and separate OCT source and fluorescence excitation light). We have shown the feasibility of this system in simultaneously visualizing tissue architectural morphologies (from the OCT

#175360 - $15.00 USD Received 7 Sep 2012; revised 15 Oct 2012; accepted 15 Oct 2012; published 16 Oct 2012

module) and fluorescent molecule distribution (from the fluorescence imaging module) in *ex vivo* rabbit esophagus samples, and the results suggest future potential of the technology for *in vivo* and possibly clinical applications.

Acknowledgments

This work was supported in part by the National Institutes of Health under grants Nos. R01CA120480 and R01EB007636.

#175360 - $15.00 USD Received 7 Sep 2012; revised 15 Oct 2012; accepted 15 Oct 2012; published 16 Oct 2012